THE ASTROPHYSICAL JOURNAL, 492:L125–L129, 1998 January 10

IMAGING AND SPECTROSCOPY OF ARCS AROUND THE MOST LUMINOUS X-RAY CLUSTER, RX J1347.5−1145[1]

KAILASH C. SAHU,[2] RICHARD A. SHAW,[2] MARY ELIZABETH KAISER,[3,4] STEFI A. BAUM,[2] HENRY C. FERGUSON,[2]
JEFFREY J. E. HAYES,[2] THEODORE R. GULL,[3] ROBERT J. HILL,[5] JOHN B. HUTCHINGS,[6]
RANDY A. KIMBLE,[3] PHILIP PLAIT,[7] AND BRUCE E. WOODGATE[3]
Received 1997 August 7; accepted 1997 October 30; published 1997 December 30

ABSTRACT

The cluster RX J1347.5−1145, the most luminous cluster in the X-ray wavelengths, was imaged with the newly installed Space Telescope Imaging Spectrograph (STIS) on board the *Hubble Space Telescope*. Its relatively high redshift (0.451) and luminosity indicate that this is one of the most massive of all known clusters. The STIS images unambiguously show several arcs in the cluster. The largest two arcs (>5″ length) are symmetrically situated on opposite sides of the cluster, at a distance of ~35″ from the central galaxy. The STIS images also show approximately 100 faint galaxies within the radius of the arcs whose combined luminosity is $\sim 4 \times 10^{11}\ L_{\odot}$. We also present ground-based spectroscopic observations of the northern arc that show one clear emission line at ~6730 Å, with a very faint continuum on either side. The emission line is consistent with an identification as [O II] λ3727, implying a redshift of 0.81 for this arc. The southern arc shows a faint continuum but no emission features. The surface mass within the radius of the arcs (240 kpc), as derived from the gravitational lensing, is $\sim 6.3 \times 10^{14}\ M_{\odot}$. The resultant mass-to-light ratio of ~1200 is higher than what is seen in many clusters but smaller than the value recently derived for some "dark" X-ray clusters (Hattori et al.). The total surface mass derived from the X-ray flux within the radius of the arcs is $\sim (2.1\text{–}6.8) \times 10^{14}\ M_{\odot}$, which implies that the ratio of the gravitational to the X-ray mass is ~1–3. The surface *gas* mass within this radius is $\sim 3.5 \times 10^{13}\ M_{\odot}$, which implies that at least 6% of the total mass within this region is baryonic.

Subject headings: dark matter — galaxies: clusters: individual (RX J1347.5−1145) — gravitational lensing

1. INTRODUCTION

Clusters of galaxies are the most massive gravitationally bound systems in the universe. They serve as important probes of the large-scale structures and their evolution (see, e.g., Bahcall 1988). An accurate mass determination of such clusters can place very useful constraints on Ω and the nature of the dark matter (White & Fabian 1995).

RX J1347.5−1145 [R.A. (2000) = $13^{h}47^{m}30\overset{s}{.}5$, decl. (2000) = $-11^{\circ}45'09''$] is the most luminous X-ray cluster among all the clusters observed in the *ROSAT* all-sky survey (Schindler et al. 1995). Its high luminosity, coupled with a redshift of 0.451, implies that this is one of the most massive of all clusters known to date.

The cluster has two optically bright galaxies at the center. Optical spectra for these brightest cluster members indicate that the cluster is at a redshift of $z = 0.451$ (Schindler et al. 1995). Optical images obtained by Schindler et al. (1995) and Fischer & Tyson (1997) show two possible bright arcs symmetrically situated ~35″ away from the brightest cluster member and some hint of other arcs, requiring higher spatial resolution images for confirmation. Spectral observations for the arcs were not available. This Letter presents high spatial resolution images obtained with the Space Telescope Imaging Spectrograph (STIS), and ground-based spectroscopic observations for the arc, which are used to estimate the mass of the cluster.

2. MASS DISTRIBUTION FROM X-RAY OBSERVATIONS

Many of the X-ray–bright clusters show the presence of gravitationally lensed arcs. From an optical follow-up study of 41 X-ray–bright clusters, Gioia & Luppino (1994) show that, compared with an optically selected sample, the X-ray selected sample has a 3 times larger probability of showing gravitationally lensed arcs. This indicates clearly that the luminous X-ray clusters are massive, perhaps the most massive of all observed objects in the universe. Their total mass determination is clearly important, and their mass profile may give important clues to the nature of the dark matter.

These X-ray clusters provide an opportunity not only to study these most massive members of the universe, but also to study the properties of background galaxies imaged as arcs. The gravitational lensing facilitates this study in two important ways. First, it provides a direct way to derive the mass of the lensing cluster. Second, it increases the brightness of the background galaxy by the formation of the arcs, thereby enabling us to study the background galaxy that would have otherwise been too faint.

In the *ROSAT* band of 0.1–2.4 keV, the X-ray emission from RX J1347.5−1145 extends to a radius of ~4.′2, with an observed luminosity of 7.3×10^{45} ergs s^{-1} within this radius. The *ASCA* observations (2–10 keV) show emission out to a radius of ~6.′4, with an observed luminosity of 4.6×10^{45} ergs s^{-1} in this band. From the X-ray observations, the mass distributions within radii of 240 kpc, 1 Mpc, and 3 Mpc have been derived. The total surface mass within the radius of the large arcs (240 kpc) is $2.1 \times 10^{14}\ M_{\odot}$. Within a radius of 1

[1] Based on observations with the NASA/ESA *Hubble Space Telescope*, obtained at the Space Telescope Science Institute, which is operated by AURA, Inc., under NASA contract NAS5-26555, and the 3.6 m telescope of the European Southern Observatory at La Silla, Chile.

[2] Space Telescope Science Institute, 3700 San Martin Drive, Baltimore, MD 21218.
[3] NASA Goddard Space Flight Center, Code 681, Greenbelt, MD 20771.
[4] Department of Physics and Astronomy, Johns Hopkins University, Baltimore, MD 21218.
[5] Hughes STX Corporation, NASA Goddard Space Flight Center, Code 681, Greenbelt, MD 20771.
[6] Dominion Astrophysical Observatory, National Research Council of Canada, 5071 Saanich Road, RR. 5, Victoria, British Columbia V8X 4M6, Canada.
[7] Advanced Computer Concepts, NASA Goddard Space Flight Center, Code 681, Greenbelt, MD 20771.

TABLE 1
LOG OF GROUND-BASED SPECTROSCOPIC OBSERVATIONS

Position	Date of Observation (1995 June)	Grating	Integration Time (s)	Wavelength Range (Å)	Resolution (Å)
Northern arc	28	R300	6000	6200–9600	8
	28	B300	6000	3600–6800	8
Southern arc	29	R300	6300	6200–9600	8
	29–30	B300	7200	3600–6800	8
Two central galaxies	28	R300	3600	6200–9600	8

Mpc, the gas mass is $2.0 \times 10^{14}\ M_{\odot}$, and the total mass, assuming hydrostatic equilibrium, is $5.8 \times 10^{14}\ M_{\odot}$. On the 3 Mpc scale, the gas mass is $8.9 \times 10^{14}\ M_{\odot}$, and the total mass is $1.7 \times 10^{15}\ M_{\odot}$.

3. OBSERVATIONS

The newly installed STIS on board the *Hubble Space Telescope* (*HST*) was used to obtain the images of RX J1347.5−1145. Observations were taken on 1997 May 25 with the CCD detector using the clear and the long-pass–filtered apertures (Baum et al. 1996). A mosaic of four (50″ × 50″) unfiltered CCD images was taken to encompass the field of arcs that span more than 70″. The field of view of the long-pass filter (28″ × 50″) is smaller than the clear aperture. As a consequence, only the brightest central galaxy and arc 2 were imaged with this filter. The integration times for each telescope pointing ranged from 250 to 300 s.

Spectroscopic observations were taken using the versatile, high-throughput ESO Faint Object Spectrographic Camera at the ESO 3.6 m telescope at La Silla, Chile. The camera has both imaging and spectroscopic capabilities. Since the spectrograph can hold five gratings simultaneously, multiple spectral resolutions and bandpasses were configured easily. A log of the spectroscopic observations is provided in Table 1.

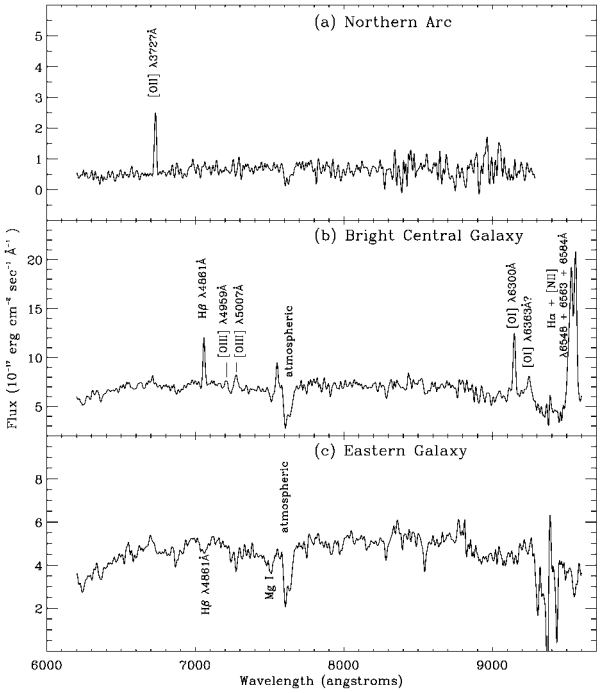

FIG. 1.—The spectra of the northern arc and the two galaxies. The region beyond 9000 Å is heavily affected by atmospheric lines. The weak features near 9000 Å in the case of the arc and the fainter galaxy are most likely due to the noise in sky subtraction. The arc shows a strong emission line at 6730 Å, the central galaxy shows many emission lines, and the eastern galaxy shows mostly absorption features.

First, a direct image of the field was obtained with an exposure of 30 s. The seeing at this time was ~1.″5. A field of view of 5.′2 × 5.′2 was obtained using the 512 × 512 pixel Tektronix CCD. A slit of 1.″5 width was used for all the observations. The first spectra were obtained with the R300 grating, with the slit oriented so that the northern arc was along the length of the slit. A single, bright emission feature at ~6730 Å with a faint continuum on either side can be seen in each of the two exposures taken in this configuration. Spectra obtained in the blue with the B300 grating did not show any additional features. The two galaxies were placed in the slit, and three exposures, each of 20 minutes duration, were taken with the R300 grating. Figure 1 shows the combined spectrum for the northern arc and the two central galaxies.

Similar observations were taken for the southern arc. However, exposures of the southern arc in the same grating setup (R300) show no trace of emission; only a faint continuum was visible. Spectra were then taken with the B300 grating that spanned the wavelength region from 3600 to 6800 Å. No features, except a faint continuum in the blue, are visible, despite the fact that the detection limit for the southern arc is better than for the northern arc. If the arc has [O II] emission at 3727 Å, then the observations indicate that it is redshifted beyond ~7500 Å and into a region where numerous atmospheric absorption lines make the detection difficult. This would indicate that the redshift is higher than 1. However, this object could also be a galaxy without any strong emission features, in which case the continuum of the galaxy is consistent with a redshift on the order of 0.8–1.5.

4. DATA REDUCTION AND RESULTS

The STIS images were analyzed using both the STScI CALSTIS and the IDT CALSTIS calibration pipelines (both of which essentially employ the same procedure as mentioned below), and consistent results were obtained. The overscan regions were first subtracted from the raw CCD images. Two readouts per *HST* telescope pointing position were employed to facilitate cosmic-ray rejection. The cosmic rays were removed using an algorithm that compares the two images and iteratively replaces pixels that deviate by more than 8 σ with an appropriately weighted minimum value of the pixel. Next, a bias image and a dark frame are subtracted from the data. This image is then flat-fielded using a ground-based calibration flat. The resulting image is then compared with the pipeline resident hot pixel table (>0.1 counts s^{-1} $pixel^{-1}$). Any residual hot pixels are then eliminated by visual inspection using a nearest neighbor interpolation algorithm.

A mosaic image was created by aligning the brightest feature in each of the overlap regions. The images were combined

TABLE 2
DETAILS OF ARCS AS SEEN IN STIS IMAGES

Arc	Length (L)[a] (arcsec)	Width (W)[a] (arcsec)	L/W	Distance from Central Galaxy (arcsec)	Arc Location R.A. (2000)	Arc Location Decl. (2000)
1	5.85	0.76	7.7	34.2	13 47 32.03	−11 44 42.1
2	2.09	0.33	6.4	31.6	13 47 31.13	−11 44 38.7
3	2.87	0.33	8.8	40.2	13 47 27.89	−11 45 08.5
4	7.81	0.50	15.6	36.3	13 47 29.26	−11 45 39.3
5	1.87	0.20	9.2	46.0	13 47 31.81	−11 45 51.7

NOTE.—Units of right ascension are hours, minutes, and seconds, and units of declination are degrees, arcminutes, and arcseconds.

[a] The STIS point-spread function is 0.″085 FWHM for the CCD and the clear aperture.

using the IRAF task IMCOMBINE, with a weighted average proportional to the exposure time for the overlapping regions, and counts normalized to a mean exposure time in the entire mosaic image. Figure 2 (Plate L27) shows the resultant mosaic image. The image shows several arcs that are marked in the figure. The two large arcs (1 and 4), situated on opposite sides of the central galaxy, are separated by about 70″; this is one of the largest separations seen in any cluster. Positional and dimensional information regarding the various arcs is given in Table 2.

The two large arcs were already seen from ground-based observations. However, due to the lower spatial resolution of the ground-based observations, the possibility that the arcs are foreground galaxies could not be ruled out (Fischer & Tyson 1997). STIS observations prove unambiguously that these are arcs with magnifications (which, to a first order, is the length-to-width ratio) ranging from 7 to 15. There are three additional features whose orientation and distance from the center are consistent with being arcs, although the possibility that these smaller arcs may be foreground galaxies cannot be eliminated.

The two central galaxies are clearly resolved. Figure 3 (Plate L28) shows an enlarged view of the central galaxy, which shows a clear jetlike structure on one side and a similar but much fainter structure on the opposite side. These structures, which may be jets or tidal tails, are about 0.″6 long, which corresponds to a length of ∼3 kpc. The FWHMs of the central and the fainter galaxies, as derived from the average Moffait and Gaussian fit to their structure in different position angles, are 0.″6 and 0.″4, respectively. The FWHM of the point sources in the field is ∼0.″085. Derived magnitudes for the two galaxies and the arcs are given in Table 3, which are consistent with those of Fischer & Tyson (1997).

The image processing software packages MIDAS and IRAF were used to reduce the spectral data obtained from the ground. After bias subtraction, the frames were flat-field corrected with an average of five flat-field images taken with the dome illuminated with a tungsten lamp. The sky was taken from both sides of the spectrum for a good sky subtraction. The resulting one-dimensional spectrum was then wavelength- and flux-calibrated. An He-Ar spectral lamp was used for wavelength calibration. For flux calibration, the standard stars HD 8879, a fast rotating Be star, and LTT 9239 were used. In the wavelength region redward of 7500 Å, there are several atmospheric emission lines, making it difficult to differentiate between these emission features and the source in this region. The resulting final spectra for the northern arc and the two galaxies are shown in Figure 1.

5. REDSHIFTS

5.1. *Central Galaxies*

The spectra for the two central galaxies (Fig. 1) are consistent with the lower resolution (15 Å) spectra published by Schindler et al. (1995). Compared with the eastern galaxy, the central galaxy is brighter by ∼0.4 mag and is also bluer. The central galaxy shows emission features of Hβ λ4861 and [O III] λλ4959, 5007, and the eastern galaxy shows a few absorption features, all of which indicate the lensing cluster to be at $z \sim 0.451$. Our higher resolution spectra also enable us to derive a velocity dispersion of 620 km s^{-1} for the central galaxy. Using the radius of the galaxy and the velocity dispersion, we derive (Binney & Tremaine 1987, p. 213) a mass of $2.4 \times 10^{11}\ M_{\odot}$ for the galaxy. However, this mass determination is valid only if the radius of the line-emitting region is the same as the observed radius of the galaxy, and if the system is virialized. If the line-emitting region is confined to a smaller region, this mass determination is not applicable. The mass of the line-emitting region itself would be lower, but, depending on the contribution of mass outside the line-emitting region, the total mass can be higher or lower.

5.2. *Arcs*

Since the redshift of the lensing cluster is 0.45, the redshift of the arcs must be higher. This implies that the rest wavelength of the northern arc's emission line seen at 6730 Å is less than 4638 Å. This eliminates the possibility that the emission line could be either of the Hβ λ4861, [O III] λλ4959, 5007, or Hα λ6563 lines. The only strong emission lines that may be responsible are the [O II] λ3727, C IV λ1550, and Lyα λ1216 lines, with corresponding redshifts of 0.8, 3.34, and 4.53, respectively. Although we cannot rule out the possibility that the emission line could be either Lyα or C IV, the color of the arc is inconsistent with this interpretation. The Lyman limit in that case would fall in the middle of the B band, and the arc would be much redder than the $B - R \sim 1.1$ value observed by Fischer & Tyson (1997).

The emission line is fully consistent with the line being the [O II] line. In that case, however, the Hβ and [O III] line emissions should be within the spectral region observed from the ground. Unfortunately, all of these lines would be hidden beneath the strong atmospheric bands that abound in this region of the spectrum. Spectra obtained with *HST* and STIS can provide an unambiguous determination of the redshift of the arc by detection of other emission lines. In our subsequent analysis, we will assume that the redshift of the arc is 0.8, noting that the mass estimate is not affected by more than 30% even if the redshift is as high as 4.

The southern arc is slightly fainter, but its distance is only about 2% larger than the distance to the northern arc. Furthermore, its center of curvature is almost centered at the bright galaxy. A simple physical model, consistent with this data and an Einstein radius equal to the distance from the center to the arc in the lens plane, predicts that the redshift of this arc is between 0.7 and 1. The lack of an emission-line detection at this wavelength suggests that either the source is a galaxy devoid of emission lines or the emission line is hidden beneath the abundance of atmospheric lines.

6. GRAVITATIONAL MASS AND THE MASS-TO-LIGHT RATIO

Fischer & Tyson (1997) have obtained a deep ground-based image of the cluster with a field size of dimension $(14')^2$, which

TABLE 3
V MAGNITUDES OF GALAXIES AND ARCS[a]

FILTER	EASTERN GALAXY	CENTRAL GALAXY	ARC 1	ARC 2	ARC 3	ARC 4	ARC 5	$(V-I)$
Clear	19.6	19.2	22.2	22.2	23.3	21.5	23.2	1.0 assumed
Long pass	...	19.2[b]	...	22.3[c]	...	...	...	0.93,[b] 1.4[c]

[a] The uncertainties in the magnitudes are 0.2 for the two galaxies and 0.4 for the arcs.
[b] The measured color term for the brightest galaxy in the field. No color information is available for the eastern cD galaxy.
[c] The measured color term for arc 2. This is the only arc for which color information can be measured.

they have used for a mass-modeling of the cluster (also see Tyson & Fischer 1995). They detect a shear signal in the background galaxies in the radial range of 35″–400″ from the cluster center and estimate the redshift of the arcs to be $1.4^{+1.4}_{-0.35}$ and $1.6^{+2.0}_{-0.5}$, respectively. Here we confine ourselves to the strong lensing regime ($r < 35''$). The fact that the two arcs on the opposite sides (arcs 1 and 4) have rather large magnifications and the center of the radius of curvature of the arcs lies close to the central galaxy makes the mass-modeling rather straightforward. In such a case, the angular radius θ_E, corresponding to the Einstein radius of the lensing galaxy R_E, can be expressed as (Schneider, Ehlers, & Falco 1990; Blandford & Narayan 1992)

$$\theta_E^2 = \frac{4GMD}{c^2}, \quad D = \frac{D_{ds}}{D_d D_s}, \tag{1}$$

where M is the mass of the lensing object, D_d is the distance to the lensing object, D_{ds} is the distance from the lens to the source, and D_s is the distance from the observer to the source (all distances being angular distances). We can assume θ_E to be the same as the distance from the lensing galaxy to the arc (34.″9 for the northern arc). Since the redshifts of the lensing galaxy and the arc are now known, we can derive the "enclosed mass." The resulting "enclosed mass" is $6.3 \times 10^{14}\ M_\odot$ (assuming $\Omega = 1$, $\Lambda = 0$, and $H_0 = 50$ km s^{-1} Mpc^{-1}).

To derive the total luminosity, we measured the fluxes of all (~100) galaxies within the radius of the assumed Einstein ring of the cluster. To derive the magnitudes in the CCD-clear aperture, we use the following formula as determined from the cycle 7 calibration programs:

$$V(\text{Johnson}) = -2.5 \log (c/s) + 25.69 + 0.479(V-I), \tag{2}$$

where c refers to counts obtained with gain = 1. Using the magnitude and color information for the two central cD galaxies (given in Table 3) and other galaxies in the field, we estimate that the combined flux from these two galaxies is approximately 38% of the total flux from all the galaxies (assuming the contribution from even fainter galaxies is small). For the luminosity distance to the cluster, we use $H_0 = 50$ km s^{-1}, and $\Omega = 0$, which gives a distance of 2800 Mpc, corresponding to a distance modulus of $(m - M) = 42.3$. Applying a K-correction of 0.6 mag appropriate for the cluster, the derived total luminosity of all the galaxies is $5 \times 10^{11}\ L_\odot$. This implies a mass-to-light ratio of 1200 within the assumed radius of the Einstein ring.

7. DISCUSSION

RX J1347.5−1145 is the most luminous X-ray cluster and one of the most massive of all clusters. We have used the STIS images and the spectroscopic information of the arcs to derive a mass of $6.3 \times 10^{14}\ M_\odot$ within the Einstein ring (240 kpc). The total surface mass within this region as derived from the X-ray observations is $2.1 \times 10^{14}\ M_\odot$ (Schindler, Hattori, & Böhringer 1996) to $6.8 \times 10^{14}\ M_\odot$ (Allen 1997). Thus, the ratio of the gravitational mass (which we can assume to be the total mass within the radius) to the X-ray mass is between 1 and 3. The surface *gas* mass within this radius, as derived from the X-ray observations, is $\sim 3.5 \times 10^{13}\ M_\odot$. We can assume this gas to be baryons, which implies that baryons contribute at least ~6% to the total mass in this central region of the cluster. Since the cluster is dominated by dark matter with a mass-to-light ratio of ~1200, this also implies that at least 6% of the *dark matter* in this region is baryonic. It is interesting to note that Hottari et al. (1997) have recently derived a mass-to-light ratio of ~3000 for a luminous X-ray cluster, where they find that the bulk of the matter is not only emitting X-rays but is also rich in metals.

From a weak-lensing model, Fischer & Tyson (1997) have derived a mass of $1.0 \times 10^{15}\ M_\odot$ within 1 Mpc (400″). As derived from the X-ray observations, the total mass within this radius is $5.8 \times 10^{14}\ M_\odot$, and the total surface mass within this radius is $1.0 \times 10^{15}\ M_\odot$ (Schindler et al. 1996). This implies that the discrepancy between the gravitational and the X-ray mass for the whole cluster is also not large. This is consistent with the ratio in the central region of the cluster found from our study. The mass-to-light ratio, as derived from the ratio of the gravitational mass to the combined luminosity from all the galaxies within the field, is 200 for the whole cluster (Fischer & Tyson 1997). This is similar to what is found in other large clusters such as Coma (Hughes 1989) but lower than what is seen in the central region of RX J1347.5−1145.

In conclusion, the discrepancy between the X-ray mass and the gravitational mass is not large in either the central or the outer part of the cluster. The cluster is dominated by dark matter, and the baryonic component in the central region is at least ~6%.

We would like to thank Mike Potter for assistance with the spectral data reduction. We thank Stella Seitz and Sabine Schindler for useful comments on the manuscript.

REFERENCES

Allen, S. W. 1997, MNRAS, in press (astro-ph/9710217)
Bahcall, N. 1988, ARA&A, 26, 631
Baum, S., et al. 1996, STIS Instrument Handbook, Version 1.0 (Baltimore: STScI)
Binney, J., & Tremaine, S. 1987, Galactic Dynamics (Princeton: Princeton Univ. Press)
Blandford, R. D., & Narayan, R. 1992, ARA&A, 30, 311
Fischer, P., & Tyson, J. A. 1997, AJ, 114, 14

Gioia, I. M., & Luppino, G. A. 1994, ApJS, 94, 583
Hattori, M., et al. 1997, Nature, 388, 146
Hughes, J. P. 1989, ApJ, 337, 21
Schindler, S., et al. 1995, A&A, 299, L9
Schindler, S., Hattori, M., & Böhringer, H. 1996, A&A, 317, 646
Schneider, P., Ehlers, J., & Falco, E. E. 1990, in Lecture Notes on Physics, Vol. 360, Gravitational Lensing, ed. Y. Mellier, B. Fort, & G. Soucail (New York: Springer), 38
Tyson, J. A., & Fischer, P. 1995, ApJ, 446, L55
White, D. A., & Fabian, A. C. 1995, MNRAS, 273, 72

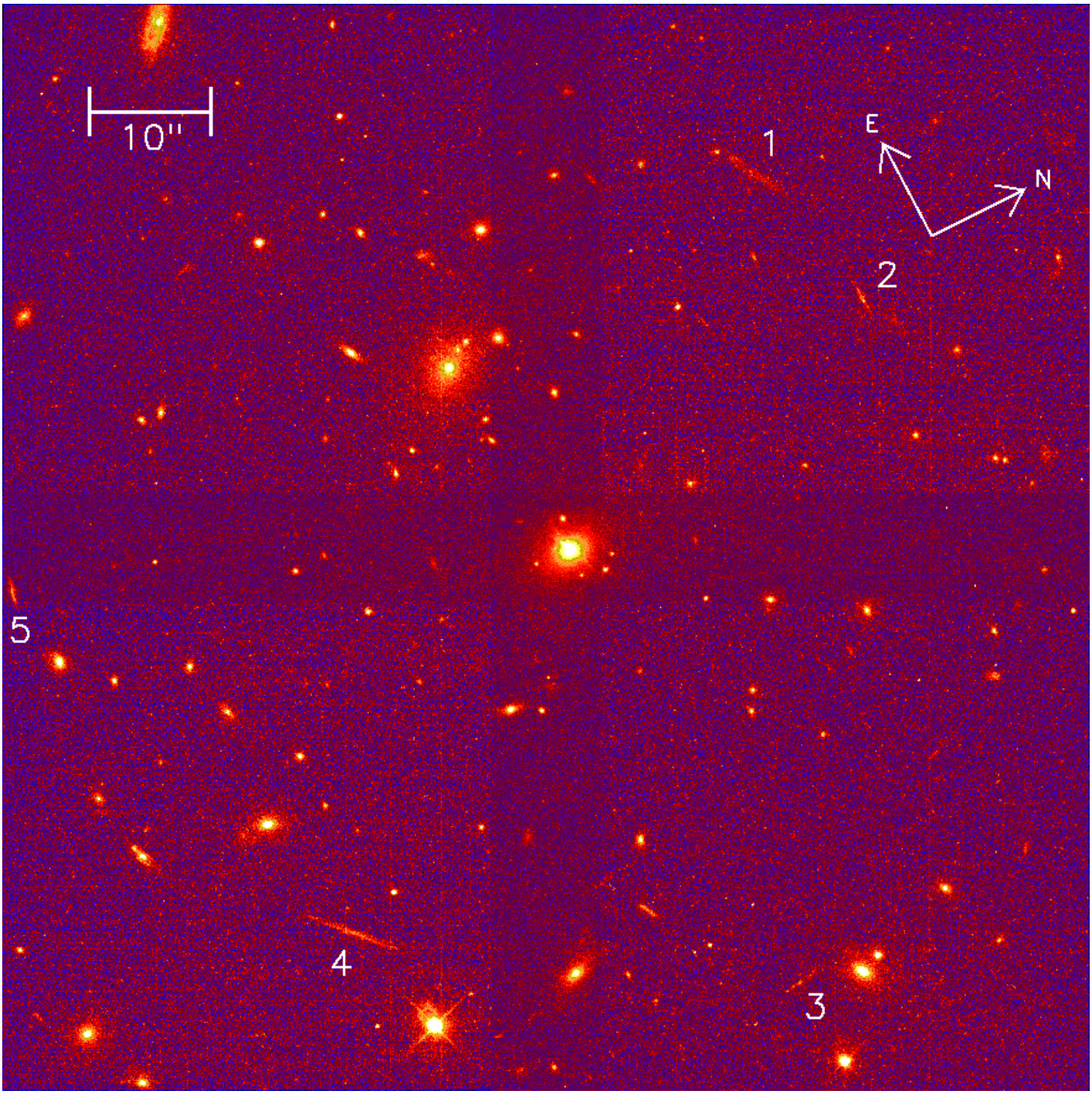

FIG. 2.—STIS mosaic image of the cluster RX J1347.5−1145 taken with the CCD and the clear filter. The central galaxy was placed in the overlapping region of all the images to increase the signal-to-noise ratio. The two large arcs (1 and 2) and other possible arcs are marked in the figure.

SAHU et al. (see 492, L127)

PLATE L27

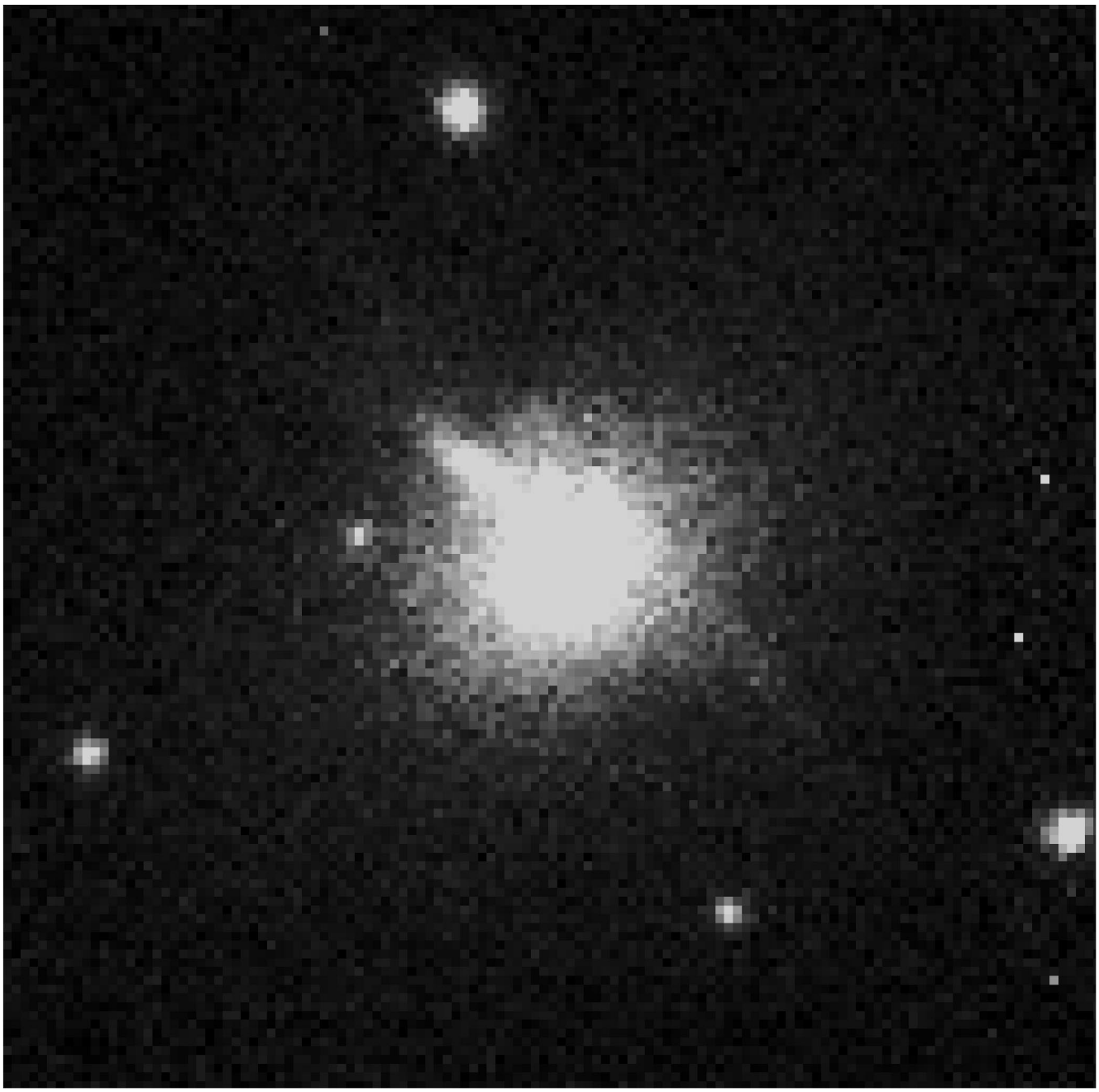

FIG. 3.—An enlarged view (6″.2 × 6″.2) of the central galaxy, which shows a clear jetlike structure on one side and a similar but much fainter structure on the opposite side. These structures, which may be jets or tidal tails, are about 0″.6 long, which corresponds to a length of ~3 kpc.

SAHU et al. (see 492, L127)